SCIENCE CHINA
Chemistry

•ARTICLES•

January 2023 Vol.66 No.1: 147–154
https://doi.org/10.1007/s11426-022-1458-4

New chiral *N*-heterocyclic olefin bifunctional organocatalysis in α-functionalization of β-ketoesters

Sijing Wang, Cefei Zhang, Da Li, Yuqiao Zhou, Zhishan Su, Xiaoming Feng & Shunxi Dong*

Key Laboratory of Green Chemistry & Technology, Ministry of Education, College of Chemistry, Sichuan University, Chengdu 610064, China

Received September 9, 2022; accepted November 10, 2022; published online December 9, 2022

N-heterocyclic olefins (NHOs) possess an electron-rich and highly polarized C=C double bond due to the donating property of nitrogen atoms. This feature imparts exocyclic carbon atom of NHOs with strong basicity and high nucleophilicity. Although NHOs have been emerging as a new type of organocatalyst and ligand for metal complexes in organic synthesis, chiral NHO-mediated highly enantioselective organic transformations were still elusive. Herein, we developed a new type of chiral amine-derived C_2-symmetric NHOs and employed them as efficient chiral bifunctional organocatalysts for asymmetric α-functionalization of β-ketoesters. With as low as 0.1 mol% catalyst loading, the desired amination and trifluoromethylthiolation products were afforded in good yields with high enantioselectivities (up to 99% yield and 99% ee). Experimental studies and theoretical calculation disclosed that hydrogen-bonding interaction upon protonation and other weak interaction between substrate and catalyst were crucial for the enantiocontrol.

organocatalyst, *N*-heterocyclic olefin, asymmetric synthesis, amination, trifluoromethylthiolation

Citation: Wang S, Zhang C, Li D, Zhou Y, Su Z, Feng X, Dong S. New chiral *N*-heterocyclic olefin bifunctional organocatalysis in α-functionalization of β-ketoesters. *Sci China Chem*, 2023, 66: 147–154, https://doi.org/10.1007/s11426-022-1458-4

1 Introduction

N-heterocyclic carbenes (NHCs) play a pivotal role in asymmetric catalysis [1]. Taking advantage of umpolung strategies, a wealth of NHCs-mediated chemical transformations were accomplished through Breslow intermediates (Scheme 1a) [2]. In contrast, their deoxy Breslow analogues, termed *N*-heterocyclic olefins (NHOs), remained largely unexplored until last decade [3]. Structurally, arising from the donating property of nitrogen atoms in NHOs, the exocyclic olefinic double bond is electron-rich and highly polarized. Therefore, NHOs possess a palpable ylide character (Scheme 1a, right), leading to the ylidic carbon atom with strong basicity and high nucleophilicity [4]. As studied by Mayr, Naumann, Ji and Cheng *et al*. [5], NHOs have comparable or stronger nucleophilicity and basicity than NHCs, and these features are closely associated with their structure. Significant advances have been made for the chemistry of NHOs within the past ten years [2–4]. On the one hand, NHOs were identified as the key intermediates for the umpolung reaction of styrenes and α,β-unsaturated carbonyls [6]. On the other hand, NHOs have been emerging as a new type of organocatalyst and ligand for metal complexes in organic synthesis. As organocatalysts, NHOs are successfully applied to several organic chemical reactions, including silylation [7], CO_2 sequestration and functionalization [5c,8] hydrosilylation/hydroborylation [7,9], transesterification [10] and heterocycle polymerization [11]. As a σ-donating type of ligands, NHOs not only enable to stabilize main group elements at low oxidation state [12], but also coordinate with transition metal salts to form well-defined complexes [4c,13]. Nevertheless, chiral NHOs were rare in the literature. The first and sole example was the hydrosilylation of acetophenone using triazole heterocycle-based chiral NHO catalyst described by Nguyen *et al*. [7] in 2017 (Scheme 1b).

Chiral α-amino acid derivatives bearing a nitrogen-

*Corresponding author (email: dongs@scu.edu.cn)

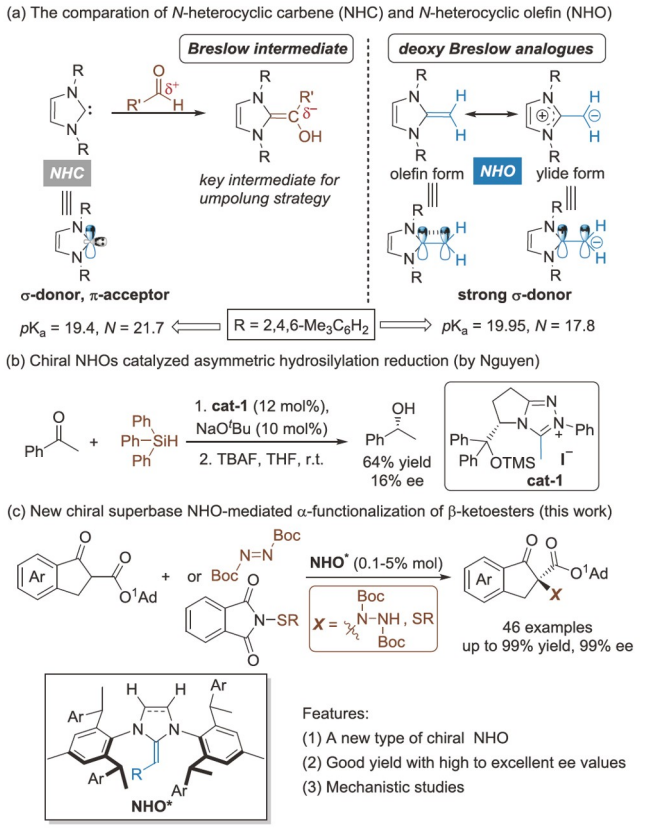

Scheme 1 The properties of NHO and its application in asymmetric synthesis (color online).

containing quaternary stereocenter are frequently occurring structure units in bioactive compounds [14]. Catalytic enantioselective α-hydrazination of 1,3-dicarbonyl compounds represent a facile and efficient route to α-amino acid derivatives. During the past two decades, several catalyst systems including transition metal-based catalysts, organic small molecule catalysts as well as frustrated Lewis pair system have been successfully established, providing various α-amino acid derivatives with good yield and high ee values [15]. In addition, due to the high lipophilicity and high electron-withdrawing character of trifluoromethylthio group, the incorporation of an SCF_3 group into small molecules is of great importance to the pharmaceutical and agrochemical industries [16]. In the past several decades, highly enantioselective methods for the construction of a stereogenic carbon center with a SCF_3 group have been documented by Shen, Rueping, Gade, Shibata *etc*. [17]. Nevertheless, there is still room for improvement in terms of new catalysts and substrate scope.

Motivated by the unique properties of NHOs and their various applications [3] in synthetic chemistry, we became curious about the design of new chiral NHOs and exploring their potential utility in asymmetric synthesis. Although NHOs were readily access from NHCs and numerous chiral NHCs have been reported, there were two obstacles associated with the development of chiral NHOs catalysis: (1) due to the long distance from the catalytic active site (exocyclic carbon atom) to the chiral backbone, the chiral induction in NHOs-mediated process was problematic [7]; (2) the addition of exogenous base for *in-situ* generation of NHOs probably led to background reaction in base-promoted chemical transformations [18]. Herein, we wish to disclose our endeavor on developing chiral NHO catalysis. Chiral amine-derived C_2-symmetric NHOs were synthesized and ultimately identified as a new type of organic bases for the asymmetric α-functionalization of β-ketoesters. With as low as 0.1 mol% of NHO organocatalyst, the desired amination adducts and sulfenylation products were afforded in good yields with high enantioselectivities (up to 99% yield and 99% ee) [19]. Based on experimental investigations and density functional theory (DFT) calculations, possible bifunctional working modes involving dual hydrogen-bond activation and other non-covalent interaction were provided to understand the enantiocontrol of the amination reaction.

2 Experimental

2.1 General procedure for catalytic asymmetric amination reaction

In a glove box, β-ketoester **1a** (0.1 mmol), di-*tert*-butyl azodicarboxylate **2a** (0.12 mmol) and **W1** (1 mol%) were added into a flame-dried Schlenk tube. Methyl *tert*-butyl ether (2.0 mL) cooled to reaction temperature was added under argon atmosphere. The resulting solution was stirred at −60 °C for 22 h. Then, the reaction mixture was subjected to column chromatography on silica gel (eluent:petroleum ether/ethyl acetate = 8/1, *v*/*v*) to afford the desired product **3aa**.

2.2 General procedure for catalytic asymmetric trifluoromethylthiolation reaction

In a glove box, β-ketoester **1a** (0.1 mmol), the SCF_3 reagent **4a** (0.12 mmol) and **W9** (1 mol%) were added into a flame-dried Schlenk tube. Methyl *tert*-butyl ether (1.0 mL) cooled to reaction temperature was added under argon atmosphere. The resulting solution was stirred at −78 °C for 22 h. Then, the reaction mixture was subjected to column chromatography on silica gel (eluent:petroleum ether/ethyl acetate = 20/1, *v*/*v*) to afford the desired product **5aa**.

3 Results and discussion

3.1 Identification of the optimized amination reaction conditions

Inspired by elegant works on C_2-symmetric NHC/metal

complex catalysis by the groups of Gawley, Shi and Cramer *et al*. [20], we envisioned that this type of NHCs might be a good candidate for synthesis of chiral NHOs (Scheme 2) since it enables to incorporate stereogenic centers in close proximity to exocyclic C=C site, which putatively was reactive center. As illustrated in Scheme 2, the reaction of free NHCs with organic halides proceeded well, affording the NHO salts in 65%−90% yield. The deprotonation of NHO salts by *t*BuOK furnished the corresponding free NHOs [21]. By variation of chiral amines, 1,2-dicarbonyls and alkyl halides, we can get a number of NHOs **W1**−**W11**. The X-ray crystal structure of **W1** indicated a close distance between terminal carbon of C=C bond and *ortho*-H of phenyl group were 2.940 and 3.066 Å, confirming our initial hypothesis.

To show the application of this new type of organocatalysts, α-amination reaction of β-ketoester **1a** with di-*tert*-butyl azodicarboxylate (**2a**) was selected as the mode reaction, and the detailed optimizations of the reaction conditions were summarized in Table 1. At the outset of our study, chiral NHO **W1** was used to investigate the reaction parameters. Performing the reaction at ambient temperature with tetrahydrofuran (THF) as the solvent provided a promising result (Table 1, entry 1, 99% yield, 66% ee). In comparison, the use of dichloromethane (DCM) instead of THF resulted in a sharp decrease of enantiomeric excess (entry 2, 4% ee). Methyl *tert*-butyl ether (MTBE) provided an increased enantioselectivity (entry 3, 80% ee *vs*. 66% ee). Decreasing the reaction temperature led to further elevated ee values at 1 mol% catalyst loading (entries 4−6, 81%−96% ee). When the reaction was run at −60 °C for 22 h, the corresponding amination product **3aa** was obtained in 99% yield with 96% ee (entry 5). Switching NHO **W1** to the related NHC **S1** resulted in inferior outcome (70% ee), indicating the important role of exocyclic C=C double bond [22]. Variation of the substitution of phenyl group at 2,6-position provided comparable results (entries 8 and 9, 94% and 92% ee, respectively). To our surprise, the structure of *N*-heterocycle had a profound effect on the enantioselectivity (entries 10−12). Chloro-substituted NHO **W4**, acenaphthenequinone derived **W5** and imidazolidine-based NHO **W6** resulted in substantial loss in yield and enantioselectivity (14%−41% yield, 2%−6% ee). In addition, the examination of the terminal substitution on the exocyclic olefin (**W7**−**W11**) were carried out as well. However, no better outcomes were obtained (see Supporting Information online, page 16 for more details). In contrast, the use of triazole derived **W12** afforded poor results (16% yield, 6% ee, see Supporting Information online, page 16 for more details) [7]. Notably, the catalyst loading can be reduced to as low as 0.1% without an obvious erosion of enantioselectivity although the longer

Table 1 Optimization of the reaction conditions for the asymmetric amination [a]

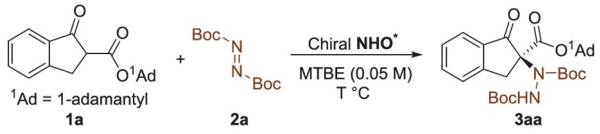

Entry	Cat*(mol%)	*T* (°C)	Yield (%)	ee (%)
1 [b]	**W1**(5)	rt	99	66
2 [c]	**W1** (5)	rt	99	4
3	**W1** (5)	rt	99	80
4	**W1** (1)	−20	92	89
5	**W1** (1)	−60	99	96
6	**W1** (1)	−78	28	81
7	**S1** (1)	−60	99	70
8	**W2** (1)	−60	96	94
9	**W3** (1)	−60	89	92
10	**W4** (1)	−20	14	2
11	**W5** (1)	−20	41	2
12	**W6** (1)	−20	32	6
13	**W1** (0.5)	−60	66	96
14	**W1** (0.1)	−60	58	96

a) Unless otherwise noted, all reactions were carried out with **1a** (0.10 mmol), **2a** (0.12 mmol) and chiral **NHO*** (1 mol%) under the given reaction conditions for 22 h. The ee was determined by high performance liquid chromatography (HPLC) analysis on a chiral stationary phase. Isolated yield. b) Tetrahydrofuran (THF) as solvent. c) Dichloromethane (DCM) as solvent. MTBE = methyl *tert*-butyl ether.

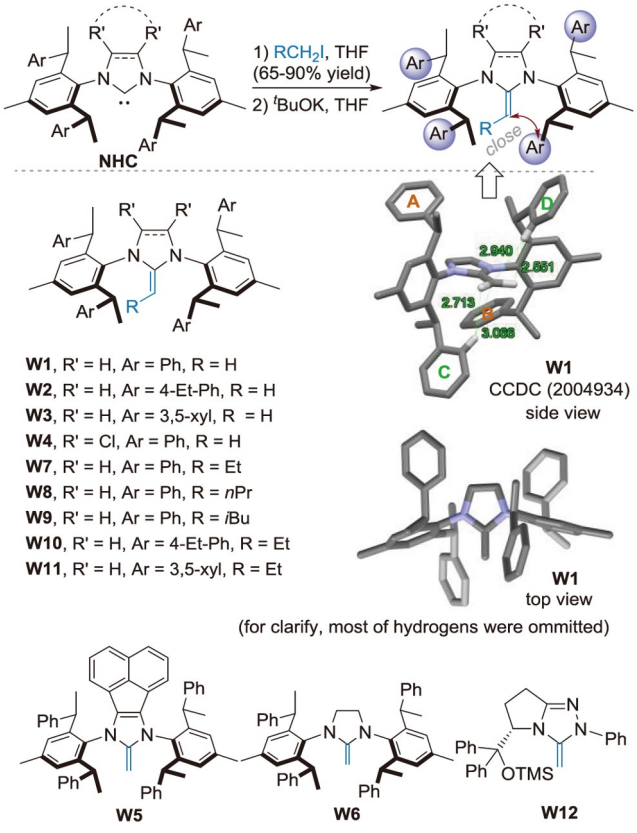

Scheme 2 The synthesis of chiral NHOs and their structure (color online).

reaction time was required (entries 13 and 14).

3.2 Substrate scope of enantioselective amination

With the standard reaction conditions in hand, the scope of β-ketoesters for the asymmetric amination reactions was evaluated. A variety of β-ketoesters **1a**−**1u** derived from indanone or tetralone were subjected to the standard conditions and the results were collected in Table 2. Indanone derived β-ketoesters **1** regardless of the electronic and steric properties of substitution on the phenyl group all proceeded well, affording the desired amination **3aa**−**3ra** in moderate to good yield with high enantiomeric purity (77%−99% yield, 89%−98% ee) except **3pa** (99% yield, 68% ee). A higher catalyst loading was needed for the reaction of 6-F substituted β-ketoester **1l**, and the related adduct **3la** was isolated in 77% yield with 98% ee. The fused substrate **1s** was compatible in the reaction system, producing the adduct **3sa** in 99% yield with 96% ee. Switching to six- and seven-membered ring derived β-ketoesters **1t** and **1u** gave a relatively lower enantioselectivity (70% ee and 68% ee) comparing with **1a**. The absolute configuration of **3wa** was assigned to be (*S*) by comparation to the optical rotation parameter in previous work [15l].

3.3 Identification of the optimized trifluoromethylthiolation reaction conditions

Intrigued by the unique properties of compounds containing SCF_3 moiety, we attempted to employ these newly developed NHOs as the promoters for asymmetric sulfenylation of β-ketoesters. As shown in Table 3, under amination conditions, the reaction of β-ketoester **1a** with "SCF_3" reagent **4a** occurred smoothly, furnishing the corresponding product **5aa** in 65% yield with 80% ee (Table 3, entry 1). Further decreasing the reaction temperature to −78 °C led to an improved enantiocontrol (entry 2, 88% ee). The attempts to heighten ee value by adjusting the substituents of phenyl moiety and structure of *N*-heterocycle were fruitless (See Supporting Information online for more details). Eventually, the terminal substitutions on the exocyclic olefin were investigated. It was delight to find that the isobutyl substituted NHO **W9** was a better candidate than *n*-propyl substituted **W7** and **W8** with *n*-butyl group (entries 3−5, 90% ee *vs*. 86% ee). Modification of phenyl group at the stereogenic centers supplied inferior results (entries 6 and 7, **W10** and **W11**, 74% and 78% ee, respectively). Thus, the optimal conditions were established with **W9** (1 mol%) in MTBE at −78 °C (entry 5).

3.4 Substrate scope of enantioselective trifluoromethylthiolation

Under the optimized conditions, the substrate scopes were evaluated to demonstrate the general utility of this asymmetric α-trifluoromethylthiolation. As shown in Table 4, the

Table 2 Scope of the enantioselective amination [a)]

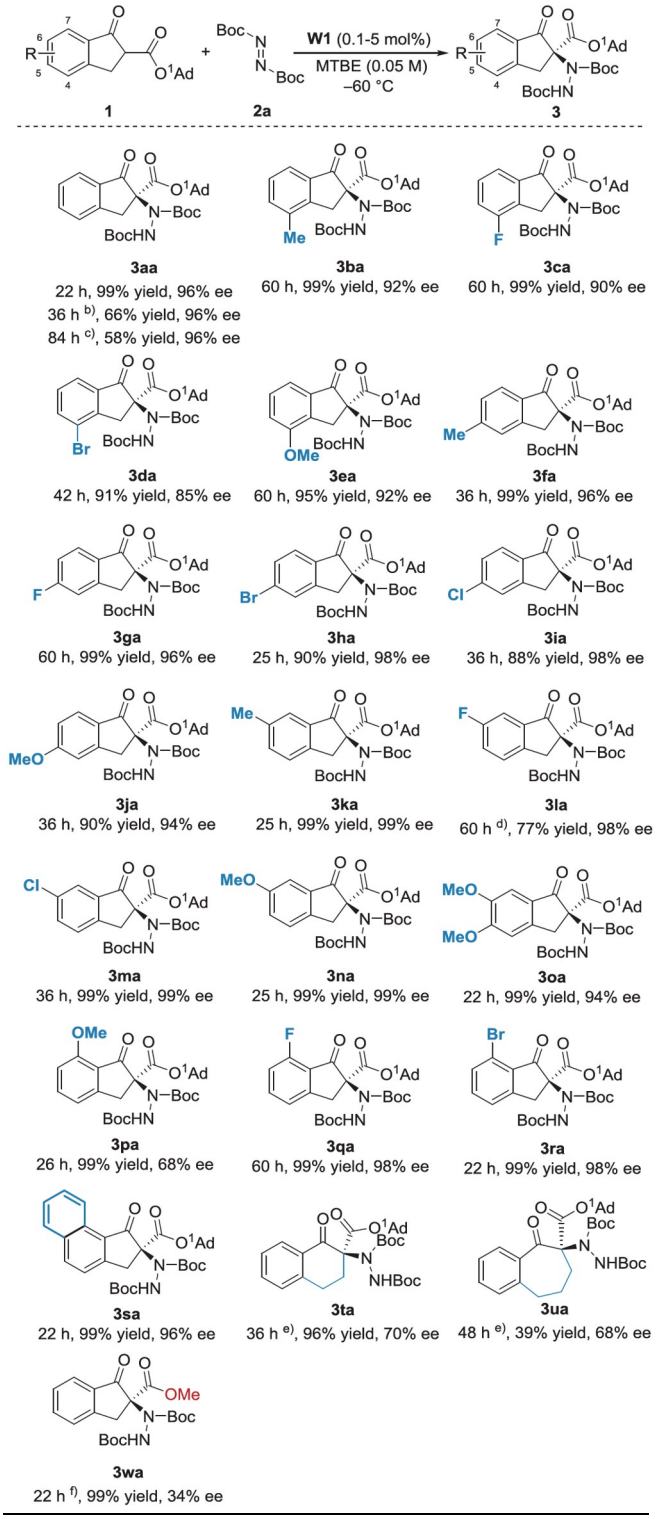

a) Unless otherwise noted, all reactions were carried out with **1** (0.10 mmol), **2** (0.12 mmol) and **W1** (1 mol%) in MTBE (0.05 M) at −60 °C. Isolated total yields of product **3**. The ee values were determined by HPLC analysis on a chiral stationary phase. b) **W1** (0.5 mol%). c) **W1** (0.1 mol%). d) **W1** (5 mol%). e) **W1** (2 mol%). f) **W7** (1 mol%).

Table 3 Optimization of the reaction conditions for the asymmetric amination [a)]

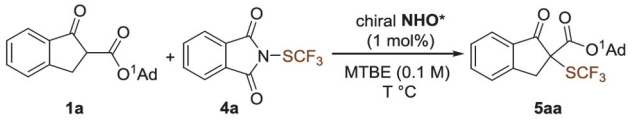

Entry	Cat*(mol%)	*T* (°C)	Yield (%)	ee (%)
1	**W1**	–60	65	80
2 [b)]	**W1**	–78	99	86
3	**W7**	–78	96	86
4	**W8**	–78	97	86
5	**W9**	–78	99	90
6	**W10**	–78	86	74
7	**W11**	–78	89	78

a) Unless otherwise noted, all reactions were carried out with **1a** (0.10 mmol), **4a** (0.12 mmol) and chiral **NHO*** (1 mol%) under the given reaction conditions for 22 h. The ee was determined by UPC^2 analysis on a chiral stationary phase. Isolated yield. b) 38 h.

substituent pattern and the electronic property of the aryl moiety have a limited effect on the reactivity and stereoselectivity. All of them were smoothly converted to the desired products **5aa**–**5ra** in good yield (82%–99%) with high enantioselectivity (74%–94% ee). Diminished ee values were obtained for naphthyl substituted **5sa** (86% yield, 58% ee) and cyclopentanone derived **5va** (72% yield, 64% ee). It was worthy of noting that six- and seven-membered ring derived β-ketoesters were suitable substrates, furnishing the related products **5ta** and **5ua** in good outcomes. In addition, cyclohexylsulfenylation and phenylsulfenylation occurred smoothly with thioaryl or thioalkyl reagent, providing the desired products **5va**, **5ab** and **5ac** in 55%–99% yield with 92%–96% ee.

3.5 Synthetic applications

To illustrate the potential synthetic application of the current methods, gram-scale synthesis of **3aa** and several transformations were carried out (Scheme 3). β-Ketoester **1a** (2 mmol) reacted smoothly with **2a** (1.2 equiv.), and the product **3aa** was isolated in 1.07 g (99% yield) with 96% ee after 72 h in the presence of 1 mol% **W1** (Scheme 3a). Removal of the terminal Boc group in **3aa** with TFA in DCM gave rise to compound **6aa** in 80% yield with maintained enantiopurity (Scheme 3b). The consecutive reduction and removal of terminal Boc group of **3aa** afforded β-hydroxyl-α-aminoester **7aa** in 62% yield with >19:1 dr and 96% ee. Treatment of **7aa** with 1,1′-carbonyldiimidazole (CDI) afforded heterocyclic product **8aa** in 61% yield without erosion of enantiomeric excess. The addition of methyl Grignard reagent to trifluoromethylthiolation adducts **5aa** and **5ja** in Et_2O at

Table 4 Scope of the enantioselective Trifluoromethylthiolation[a)]

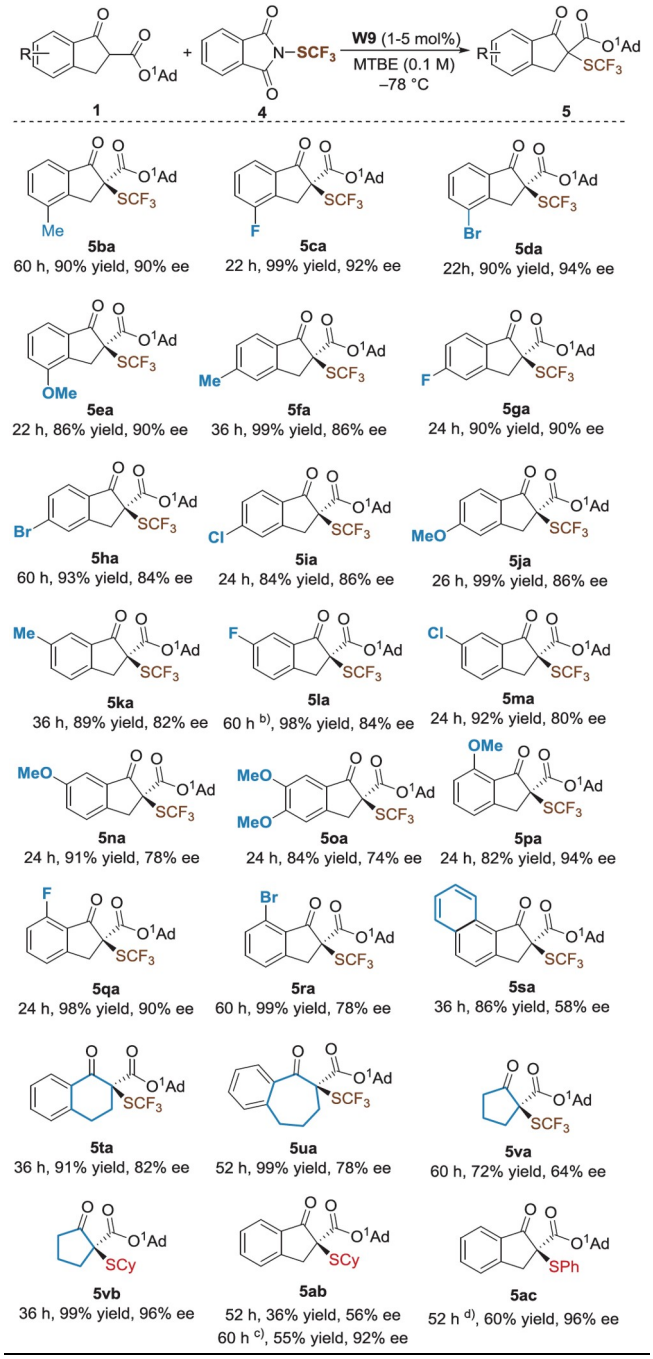

a) Unless otherwise noted, all reactions were carried out with **1** (0.10 mmol), **4** (0.12 mmol) and **W9** (1 mol%) in MTBE (0.1 M) at −78 °C. Isolated total yields of product **5**. The ee values were determined by UPC^2 analysis on a chiral stationary phase. b) **W9** (5 mol%). c) **W1** (5 mol%). d) **W9** (2 mol%).

−10 °C took place well, giving the β-hydroxyl-α-SCF_3-substituted esters **9aa** and **9ja** in high yield and excellent diastereoselectivity (Scheme 3c). The absolute configuration of **9aa** was unambiguously determined to be (1*R*,2*S*) by comparison with the optical rotation of the known compound [17e].

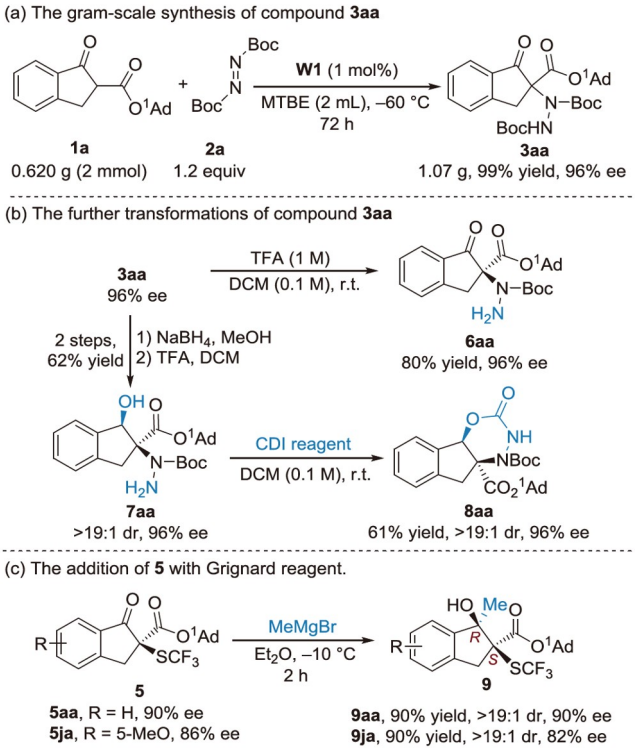

Scheme 3 The gram-scale synthesis of **3aa** and further transformations (color online).

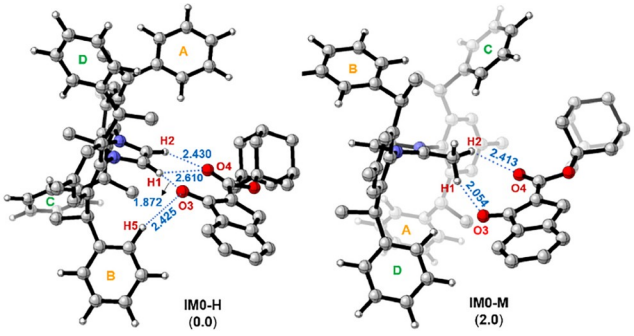

Figure 1 Optimized geometries of **IM0-H** and **IM0-M**. The relative Gibbs free energy (ΔG) was given in kcal mol^{-1} and the bond length was shown in Ångström. Four phenyl groups in **W1** were marked with A, B, C and D (color online).

3.6 Mechanism consideration

To understand the reaction mechanism and the origin of the enantiocontrol, DFT calculations at the ωB97X-D/6-311G** (SMD, THF)//B3LYP/6-31G*(SMD, THF) theoretical level using chiral NHO **W1** were performed. Due to the strong basicity of NHOs, the deprotonation of 1-adamantyl substituted β-ketoester **1a** occurred upon mixing it with NHO **W1** to give ion-pair complex, which was confirmed by ^{1}H NMR spectrum of the mixture of **1a** and **W1** (See Supporting Information online, page 83 for more details). The DFT calculation indicated that **IM0-H** with a dual hydrogen bonding interaction [23] between the two hydrogens at imidazole ring of **W1** and the oxygen atoms of enolized **1a**, was more stable than the expected **IM0-M** the Boltzmann distribution ratio of 99.14% at 213 K. The involving weak $CH_3\cdots O$ hydrogen bonding interaction in term of Gibbs free energy (Figure 1, 2.0 kcal mol^{-1}), with similar dual-hydrogen bonding interaction was observed in the X-ray crystal structure of imidazole-derived NHC salts as well [20a]. Arising from the dual-hydrogen bonding interaction with enolized β-ketoester **1a**, the chemical shift of two hydrogens at imidazole ring in ion-pair complex **IM0-H** shifted to relative down-field (9.21 ppm at 26 °C, 9.39 ppm at −20 °C) in comparation with the chemical shift (8.18 ppm) of hydrogens in NHO salt **W1•HI** (see Supporting Information online, page 84 for more details). When substrate **2a** approached **IM0-H** from its *Si* or *Re*-face alternatively, **IM1-*R*** and **IM1-*S*** were formed. In the following step, the C–N bonds in **IM2-*R*** and **IM2-*S*** were constructed *via* transition sates **TS-*R*** and **TS-*S***, respectively (Figure 2). The relative Gibbs free energy (ΔG) of **TS-*R*** was higher than that of **TS-*S*** by 2.7 kcal mol^{-1}, therefore the formation of *S*-**3aa** was favourable. Accordingly, the theoretical ee value was predicted to be 99% at 213 K, which was close to the experimental observation (86% ee in THF, see Supporting Information online, page 15). As depicted in Figure 2, the higher energy barrier of **TS-*R*** was attributed to steric repulsion between the phenyl groups (B and C) and Boc group of **2a** as well as steric repulsion between ring A and 1-adamantly group of **1a**. This unfavorable steric effect could be verified by weak interaction analysis (Figure 2). In contrast, the bulky Boc groups of **2a** in **TS-*S*** were fay away from the 1-adamantly group of **1a** with the dihedral angle D(N7-N6-C5-C8) of −3.5°, avoiding unfavorable repulsion (Figure 2). Thus, the combination of Ph group at B position of **W1** with bulky 1-adamantly group of **1a** constructed a good chiral environment, directing **2a** to attack enolized **1a** from its *Si*-face with less steric hindrance, leading to *S*-configuration product. The above results also confirmed the important role of dual hydrogen bonding interaction for chiral NHOs **W1**, since dichloro-substituted NHO **W4** and acenaphthenequinone derived **W5** without hydrogen as well imidazolidine-based NHO **W6** with four hydrogens led to significant loss of enantioselectivity (Table 1, entries 10−12, 2%−6% ee).

In addition, the pathways *via* **IM0-M** were studied as well (For more details, see Supporting Information online, page 88). The computational outcomes indicated that the corresponding **TS-*S′*** was slightly favored over **TS-*R′*** ($\Delta\Delta G$ = 0.6 kcal/mol, theoretical ee = 61% ee). According to Boltzmann distribution ratio of **IM0-M** (0.86%) and experimental results (86% ee at –60 °C in THF), we envisioned that the reaction pathway *via* **IM0-M** was unlikely.

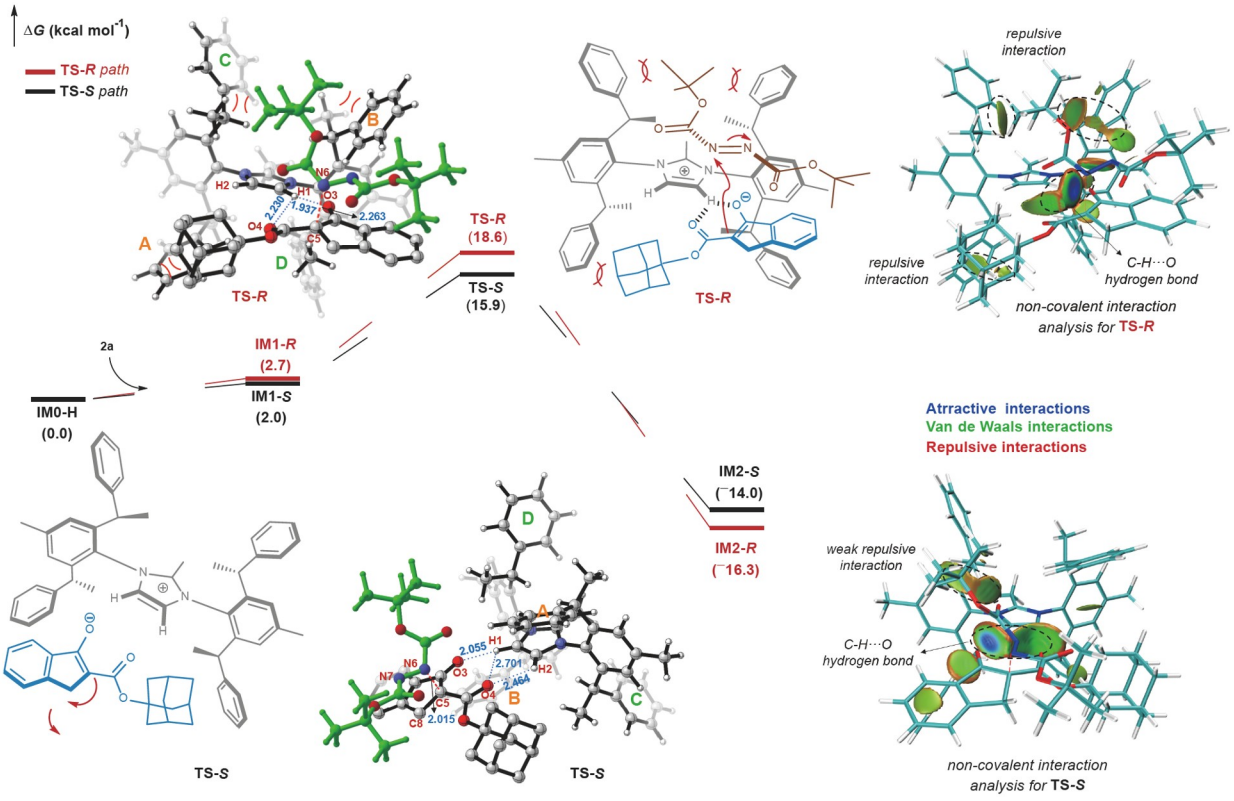

Figure 2 Energy profiles of the reaction, optimized geometries of **TS-*S*** and **TS-*R*** (gray) as well as non-covalent interaction analysis for transition states ***TS-S*** and ***TS-R*** (green). The relative Gibbs free energy (ΔG) was given in kcal mol^{-1} and the bond length was shown in Ångström (color online).

4 Conclusions

In summary, we have designed a new type of chiral NHOs catalysts and successfully applied them as bifunctional organocatalysts in the α-functionalization of β-ketoesters. With as low as 0.1% catalyst loading, the amination adducts and sulfenylation products were obtained in good yields with high enantioselectivities (up to 99% yield and 99% ee). On the basis of control experiments and theoretical calculation, a possible base and dual hydrogen-bonding bifunctional activation mode was provided to understand the origin of stereoselectivity. We anticipate that this proof-of-principle study provides a solid basis for the development of chiral NHO catalysis. The further application of chiral NHOs as organocatalysts and ligands in asymmetric synthesis is undergoing in our lab.

Acknowledgements This work was supported by the National Natural Science Foundation of China (92056107, 22271199, 21801175) and the Sichuan University (2020SCUNL204).

Conflict of interest The authors declare no conflict of interest.

Supporting information The supporting information is available online at chem.scichina.com and link.springer.com/journal/11426. The supporting materials are published as submitted, without typesetting or editing. The responsibility for scientific accuracy and content remains entirely with the authors.

1 For selected reviews of NHCs, see: (a) Enders D, Balensiefer T. *Acc Chem Res*, 2004, 37: 534–541; (b) Enders D, Niemeier O, Henseler A. *Chem Rev*, 2007, 107: 5606–5655; (c) Dröge T, Glorius F. *Angew Chem Int Ed*, 2010, 49: 6940–6952; (d) Dwivedi S, Gupta S, Das S. *COCAT*, 2014, 1: 13–39; (e) Vivancos Á, Segarra C, Albrecht M. *Chem Rev*, 2018, 118: 9493–9586; (f) Bellotti P, Koy M, Hopkinson MN, Glorius F. *Nat Rev Chem*, 2021, 5: 711–725

2 For selected reviews on NHC catalysis *via* Breslow intermediates, see: (a) Nair V, Vellalath S, Babu BP. *Chem Soc Rev*, 2008, 37: 2691–2698; (b) Biju AT, Kuhl N, Glorius F. *Acc Chem Res*, 2011, 44: 1182–1195; (c) Mahatthananchai J, Bode JW. *Acc Chem Res*, 2014, 47: 696–707; (d) Flanigan DM, Romanov-Michailidis F, White NA, Rovis T. *Chem Rev*, 2015, 115: 9307–9387

3 For selected reviews of NHOs, see: (a) Crocker RD, Nguyen TV. *Chem Eur J*, 2016, 22: 2208–2213; (b) Roy MMD, Rivard E. *Acc Chem Res*, 2017, 50: 2017–2025; (c) Naumann S. *Chem Commun*, 2019, 55: 11658–11670; (d) Liang Q, Song D. *Dalton Trans*, 2022, 51: 9191–9198

4 For selected examples of structure and properties of NHOs, see: (a) Gruseck U, Heuschmann M. *Chem Ber*, 1987, 120: 2053–2064; (b) Fürstner A, Alcarazo M, Goddard R, Lehmann C. *Angew Chem Int Ed*, 2008, 47: 3210–3214; (c) Ibrahim Al-Rafia SM, Malcolm AC, Liew SK, Ferguson MJ, McDonald R, Rivard E. *Chem Commun*, 2011, 47: 6987–6989; (d) Wang KM, Yan SJ, Lin J. *Eur J Org Chem*, 2014, 2014(6): 1129–1145; (e) Powers K, Hering-Junghans C, McDonald R, Ferguson MJ, Rivard E. *Polyhedron*, 2016, 108: 8–14

5 For selected examples of comparison of properties between NHOs and NHCs, see: (a) Maji B, Horn M, Mayr H. *Angew Chem Int Ed*, 2012,

51: 6231–6235; (b) Schuldt R, Kästner J, Naumann S. *J Org Chem*, 2019, 84: 2209–2218; (c) Wang Z, Niu QH, Xue XS, Ji P. *J Org Chem*, 2020, 85: 13204–13210; (d) Li Z, Ji P, Cheng JP. *J Org Chem*, 2021, 86: 2974–2985
6 For a review, see: (a) Nguyen XB, Nakano Y, Lupton DW. *Aust J Chem*, 2020, 73: 1–8; (b) Fischer C, Smith SW, Powell DA, Fu GC. *J Am Chem Soc*, 2006, 128: 1472–1473; (c) Matsuoka S, Ota Y, Washio A, Katada A, Ichioka K, Takagi K, Suzuki M. *Org Lett*, 2011, 13: 3722–3725; (d) Biju AT, Padmanaban M, Wurz NE, Glorius F. *Angew Chem Int Ed*, 2011, 50: 8412–8415; (e) Scott L, Nakano Y, Zhang C, Lupton DW. *Angew Chem Int Ed*, 2018, 57: 10299–10303; (f) Ito S, Fujimoto H, Tobisu M. *J Am Chem Soc*, 2022, 144: 6714–6718
7 Kaya U, Tran UPN, Enders D, Ho J, Nguyen TV. *Org Lett*, 2017, 19: 1398–1401
8 For selected examples of CO_2 sequestration and functionalization catalyzed by NHOs, see: (a) Wang YB, Wang YM, Zhang WZ, Lu XB. *J Am Chem Soc*, 2013, 135: 11996–12003; (b) Wang YB, Sun DS, Zhou H, Zhang WZ, Lu XB. *Green Chem*, 2015, 17: 4009–4015; (c) Maji S, Das A, Mandal SK. *Chem Sci*, 2021, 12: 12174–12180
9 (a) Hering-Junghans C, Watson IC, Ferguson MJ, McDonald R, Rivard E. *Dalton Trans*, 2017, 46: 7150–7153; (b) Zhang Z, Huang S, Huang L, Xu X, Zhao H, Yan X. *J Org Chem*, 2020, 85: 12036–12043
10 Blümel M, Noy JM, Enders D, Stenzel MH, Nguyen TV. *Org Lett*, 2016, 18: 2208–2211
11 For selected examples of polymerization catalyzed by NHOs, see: (a) Jia YB, Wang YB, Ren WM, Xu T, Wang J, Lu XB. *Macromolecules*, 2014, 47: 1966–1972; (b) Naumann S, Thomas AW, Dove AP. *Angew Chem Int Ed*, 2015, 54: 9550–9554; (c) Wang Q, Zhao W, Zhang S, He J, Zhang Y, Chen EYX. *ACS Catal*, 2018, 8: 3571–3578
12 For selected examples of NHOs stabilized main group elements, see: (a) Al-Rafia SMI, Momeni MR, McDonald R, Ferguson MJ, Brown A, Rivard E. *Angew Chem Int Ed*, 2013, 52: 6390–6395; (b) Roy MMD, Ferguson MJ, McDonald R, Zhou Y, Rivard E. *Chem Sci*, 2019, 10: 6476–6481; (c) Varava P, Dong Z, Scopelliti R, Fadaei-Tirani F, Severin K. *Nat Chem*, 2021, 13: 1055–1060
13 For selected examples of NHOs coordinated with transition metal salts, see: (a) Iglesias M, Iturmendi A, Sanz Miguel PJ, Polo V, Pérez-Torrente JJ, Oro LA. *Chem Commun*, 2015, 51: 12431–12434; (b) Rufh SA, Goudreault AY, Foscato M, Jensen VR, Fogg DE. *ACS Catal*, 2018, 8: 11822–11826; (c) Fischer M, Roy MMD, Hüller S, Schmidtmann M, Beckhaus R. *Dalton Trans*, 2022, 51: 10690–10696
14 (a) Venkatraman J, Shankaramma SC, Balaram P. *Chem Rev*, 2001, 101: 3131–3152; (b) Gante J. *Angew Chem Int Ed Engl*, 1994, 33: 1699–1720; (c) Schoepp DD, Jane DE, Monn JA. *Neuropharmacology*, 1999, 38: 1431–1476
15 For reviews on the amination of carbonyls, see: (a) Janey JM. *Angew Chem Int Ed*, 2005, 44: 4292–4300; (b) Vallribera A, Maria Sebastian R, Shafir A. *Curr Org Chem*, 2011, 15: 1539–1577; (c) Govender T, Arvidsson PI, Maguire GEM, Kruger HG, Naicker T. *Chem Rev*, 2016, 116: 9375–9437; (d) Usman M, Zhang XW, Wu D, Guan ZH, Liu WB. *Org Chem Front*, 2019, 6: 1905–1928; (e) O'Neil LG, Bower JF. *Angew Chem Intl Edit*, 2021, 60: 25640–25666; (f) Marigo M, Juhl K, Jørgensen KA. *Angew Chem Int Ed*, 2003, 42: 1367–1369; (g) Foltz C, Stecker B, Marconi G, Bellemin-Laponnaz S, Wadepohl H, Gade LH. *Chem Commun*, 2005, 5115; (h) Terada M, Nakano M, Ube H. *J Am Chem Soc*, 2006, 128: 16044–16045; (i) He R, Wang X, Hashimoto T, Maruoka K. *Angew Chem Int Ed*, 2008, 47: 9466–9468; (j) Yang Z, Wang Z, Bai S, Shen K, Chen D, Liu X, Lin L, Feng X. *Chem - Eur J*, 2010, 16: 6632–6637; (k) Xiao X, Lin L, Lian X, Liu X, Feng X. *Org Chem Front*, 2016, 3: 809–812; (l) Benavent L, Puccetti F, Baeza A, Gómez-Martínez M. *Molecules*, 2017, 22: 1333; (m) Wang Y, Yihuo A, Wang L, Dong S, Feng X. *Sci China Chem*, 2022, 65: 546–553
16 (a) Leroux F, Jeschke P, Schlosser M. *Chem Rev*, 2005, 105: 827–856; (b) Manteau B, Pazenok S, Vors JP, Leroux FR. *J Fluorine Chem*, 2010, 131: 140–158
17 For related reviews, see: (a) Chu L, Qing FL. *Acc Chem Res*, 2014, 47: 1513–1522; (b) Shao X, Xu C, Lu L, Shen Q. *Acc Chem Res*, 2015, 48: 1227–1236; (c) Xu XH, Matsuzaki K, Shibata N. *Chem Rev*, 2015, 115: 731–764; (d) Yang X, Wu T, Phipps RJ, Toste FD. *Chem Rev*, 2015, 115: 826–870; (e) Wang X, Yang T, Cheng X, Shen Q. *Angew Chem Int Ed*, 2013, 52: 12860–12864; (f) Bootwicha T, Liu X, Pluta R, Atodiresei I, Rueping M. *Angew Chem Int Ed*, 2013, 52: 12856–12859; (g) Deng QH, Rettenmeier C, Wadepohl H, Gade LH. *Chem Eur J*, 2014, 20: 93–97; (h) Zhang H, Leng X, Wan X, Shen Q. *Org Chem Front*, 2017, 4: 1051–1057; (i) Kondo H, Maeno M, Sasaki K, Guo M, Hashimoto M, Shiro M, Shibata N. *Org Lett*, 2018, 20: 7044–7048; (j) Tan Q, Chen Q, Zhu Z, Liu X. *Chem Commun*, 2022, 58: 9686–9689; (k) Jiang Z, Pan Y, Zhao Y, Ma T, Lee R, Yang Y, Huang KW, Wong MW, Tan CH. *Angew Chem Int Ed*, 2009, 48: 3627–3631
18 Blümel M, Crocker RD, Harper JB, Enders D, Nguyen TV. *Chem Commun*, 2016, 52: 7958–7961
19 As suggested by one reviewer, a detailed comparison of current method with other catalyst system was provided in SI, page 152
20 For selected examples of synthesis and applications of chiral amine-derived NHCs, see: (a) Albright A, Eddings D, Black R, Welch CJ, Gerasimchuk NN, Gawley RE. *J Org Chem*, 2011, 76: 7341–7351; (b) Spahn E, Albright A, Shevlin M, Pauli L, Pfaltz A, Gawley RE. *J Org Chem*, 2013, 78: 2731–2735; (c) Diesel J, Finogenova AM, Cramer N. *J Am Chem Soc*, 2018, 140: 4489–4493; (d) Cai Y, Yang XT, Zhang SQ, Li F, Li YQ, Ruan LX, Hong X, Shi SL. *Angew Chem Int Ed*, 2018, 57: 1376–1380; (e) Wang ZC, Gao J, Cai Y, Ye X, Shi SL. *CCS Chem*, 2022, 4: 1169–1179
21 (a) Knappke CEI, Neudörfl JM, von Wangelin AJ. *Org Biomol Chem*, 2010, 8: 1695–1705; (b) Knappkea CEI, Arduengo AJ, Jiao HJ, Neudörfla JM, Wangelin A-JV. *Synthesis*, 2011, 23: 3784–3795
22 (a) Chan A, Scheidt KA. *J Am Chem Soc*, 2008, 130: 2740–2741; (b) Taylor JE, Daniels DSB, Smith AD. *Org Lett*, 2013, 15: 6058–6061; (c) Santra S, Maji U, Guin J. *Org Lett*, 2022, 22: 468–473
23 Doyle AG, Jacobsen EN. *Chem Rev*, 2007, 107: 5713–5743